Macromolecules **1985**, *18*, 2380–2389

Effect of Polyacetylene Molecular Weight and Dopant Concentration on the Temperature Dependence of Transport Properties

James C. W. Chien,* John M. Warakomski, Frank E. Karasz, and Michael A. Schen

Department of Chemistry and Department of Polymer Science and Engineering, Materials Research Laboratory, University of Massachusetts, Amherst, Massachusetts 01003.
Received March 7, 1985

ABSTRACT: The transport properties of $[CH]_x$ with number-average molecular weight, M_n, from 500 to 870 000 have been studied. The room temperature conductivity, σ_{RT}, of undoped *cis*-$[CH]_x$ is nearly independent of molecular weight, MW. There is a definite trend of decrease in σ_{RT} and increase in thermopower, $\mathcal{S}_{RT}$, with increasing MW for undoped *trans*-$[CH]_x$. There is a sharp increase in σ_{RT} upon iodine doping of *cis*-$[CH]_x$ with a midpoint of $y_m(I_3^-) \sim 3 \times 10^{-5}$ for M_n 500 *cis*-$[CH]_x$, where y is the mole of dopant/CH, as compared to $y_m(I_3^-) \sim 3 \times 10^{-4}$ for $[CH]_x$ of 11 000 M_n. The latter has $y_m(I_3^-) \sim 1.6 \times 10^{-4}$ in the variation of $\mathcal{S}_{RT}$ with y. There are similar sharp increases of σ_{RT} of *trans*-$[CH]_x$ with doping. For M_n 500 polymer the transition occurs at $\sim 8 \times 10^{-5}$, which is lower than the $y_m \sim 7 \times 10^{-4}$ for M_n 11 000 *trans*-$[CH]_x$. Temperature dependence of σ has been measured down to 78 K. The data were plotted according to log σ vs. log T, $T^{-1/4}$, $T^{-1/2}$, and T^{-1}; the first type of plot is linear over a wider temperature range than the others in the order given. The slopes of these plots are found to be linearly related to $y^{1/3}$, which implies that the determinant for the temperature dependence of transport properties is the average distance separating the charge carriers and the distance between counterions. These results are consistent with our proposed model that at low dopant level the positively charged carriers are immobile due to the Coulomb interaction with the counterion. At y_m this pinning potential is completely screened and a carrier interacts equally and weakly with two or more counterions. This gives rise to a transition of the carriers in a "glassy" state with low mobility to a "melt" state with greatly increased mobility for three-dimensional variable range hopping.

Introduction

Undoped polyacetylene has room temperature conductivity, σ_{RT}, of 10^{-8}–10^{-5} $(\Omega\ cm)^{-1}$ and 10^{-9}–10^{-11} $(\Omega\ cm)^{-1}$, respectively, for the *trans*- and *cis*-$[CH]_x$.[1] Doping increases σ_{RT} of both polymers[2] to 10^2 $(\Omega\ cm)^{-1}$ or greater. From the thermopower coefficient, $\mathcal{S}$, of undoped $[CH]_x$ and *p*-doped polymers,[3] the carriers are shown to be positively charged. However, after several years of intensive investigation there are several important aspects of carrier transport in undoped and doped $[CH]_x$ that are still incompletely resolved or understood.

There have been reports on the critical dopant concentration, y_c, for attaining metallic conductivity as deduced from plots of log σ_{RT} vs. y,[4] where y is the mole of dopant/CH. The early results indicate $y_c \geq 10^{-2}$; however, there are very few data at very low dopant level. We have used isotopic $^{125}I_2$ to measure the effect of dopant at ppm level on σ_{RT}[5] and found the 10^8- to 10^{12}-fold increase to occur at a midpoint of $y_m \sim 7 \times 10^{-4}$. This phenomenon has been referred to by us as the carrier mobility transition, y_m, or carrier "glass" transition. The thermopower coefficient of undoped *trans*-$[CH]_x$ is said to be ca. 900 $\mu V\ K^{-1}$.[3,6] The decrease of $\mathcal{S}$ with AsF_5[6,7] and $FeCl_4$ doping[8] gave $y_c \sim 10^{-2}$. However, more extensive I_2 doping studies[5] show that most of the decrease in $\mathcal{S}$ occurs within 2-fold increase of dopant concentration and that $y_m \sim 7 \times 10^{-4}$, as above. What does this low value of y_m teach us about the transport mechanism?

Various mechanisms of carrier transport differ in the temperature dependence of conductivity.[1] Some of the common ones are (a) log $\sigma \propto aT^{-1}$ for activated hopping to extended states or in band tails or for the polaron hopping; (b) log $\sigma \propto bT^{-1/2}$ for 1-D variable range hopping (VRH) or fluctuation-induced tunneling (FIT) for small volume fraction of metallic islands; (c) log $\sigma \propto cT^{-1/4}$ for 3-D VRH or FIT for large volume fraction of metallic islands; and (d) log $\sigma \propto$ log T^d for intersoliton electron hopping (IEH), where a, b, c and d are the slopes of the respective plots. There have been only a few reports on $\sigma(T)$ such as on undoped *trans*-$[CH]_x$[6,9] and lightly iodine-doped *trans*-$[CHI_y]_x$ for unknown value of y.[9] Other works concentrated on heavily iodine-doped *trans*-$[CH]_x$.[10] In all these cases, with one exception,[9] the data were analyzed according to one particular $\sigma(T)$ function or another. One would think since doping greatly changes σ, $\sigma(T)$ should depend strongly on y. Yet no systematic measurements had been reported on this interdependence.

Finally, though dimensionality of the system determines the form of $\sigma(T)$ for some of the models, there does not seem to be any definitive way to elucidate this point because the molecular weight, MW, of the polymer is unknown.

Several developments in our laboratory and elsewhere open up opportunity to examine the above-mentioned questions concerning $\sigma(T,y)$. The first is the use of very slow doping of $[CH]_x$ to achieve nearly homogeneous distribution of dopants. $^{125}I_2$ was used to determine y from ppm to parts per thousand; higher levels of doping up to saturation were obtained from weight uptake.[5,11] Results for y for overlapping regimes were in excellent agreement. A method was developed to determine the number-average molecular weight, M_n, of $[CH]_x$ by using isotopic CH_3OH^* tagging of the chain.[12] The use of isotopic CO^* and C^*O_2 with the propagating chain yielded the catalytic active sites concentration in acetylene polymerization[13] and the kinetic rate constants. The results afforded rational choice of polymerization conditions for the synthesis of $[CH]_x$ with M_n values from 400 to 920 000. The synthesis procedures, characterization, and thermal isomerization of different MW $[CH]_x$,[14] a brief description of their electrical conductivity,[15] and a detailed report on the effect of MW on their magnetic properties[16] have been published. The central purpose of this work is to measure in great detail the transport properties of *cis*- and *trans*-$[CH(I_2)_y]_x$ for $10^{-6} < y < 10^{-1}$ as a function of temperature for polymers with $400 \leq M_n \leq 920\,000$.

Materials and Techniques

Polymerization. Three different MW types of polyacetylene were synthesized. The standard 100-μm film sample of S-*cis*-$[CH]_x$ was prepared according to the procedure of Ito et al.,[17] which

0024-9297/85/2218-2380$01.50/0

has M_n = 11 000. Using high $Ti(OBu)_4$ concentration of about 0.2 M, Al/Ti = 7 to increase chain transfer rate, no catalyst aging, low $p_{C_2H_2}$ = 20–30 torr to reduce propagation rate, 195 K, and polymerization time of 2 h, we obtained very low MW **L**-*cis*-$[CH]_x$ with M_n = 400–500.[14] For polymerization of acetylene to high MW, we used $[Ti(OBu)_4]_0 \leq 1$ mM, Al/Ti = 4, $p_{C_2H_2} \geq 760$ torr, catalyst aging 30–60 min, temperature 263 K, and polymerization time of 2 h to produce **H**-*cis*-$[CH]_x$-(N), where N is $M_n \times 10^{-4}$. Polymers with N from 2.1 to 92 were obtained.[14] The values of M_n were determined by radiotagging.[12]

Acetylene was also directly polymerized in the four-probe apparatus used to measure conductivity so that the polymer was never exposed to air. Half of a thin microscope cover slide was mounted on the leads of the four-probe with a little Electrodag on each wire. The four-probe apparatus was modified for use as a polymerization reactor with Ar and C_2H_2 inlets and a resevoir containing solvent. Ten milliliters of catalyst was introduced. Shaking the vessel covered the slide with a thin layer of the catalyst solution. A film of $[CH]_x$ was formed on the slide during the polymerization. The conductivity of $[CH]_x$ was followed as it was washed and thoroughly isomerized.

Doping. A piece of $[CH]_x$ film was mounted on the four-probe wires with Electrodag 502 (Acheson Colloids Co.) in the drybox. Two large pieces (ca. 20–50 mg) of polyacetylene were placed in the vessel, one to determine iodine weight gain and the other piece was used for measurements. A tube (0.8 × 12 cm) with a Teflon stopcock on top and #7 O-ring joint on the side serves as a reservoir for several hundred milligrams of iodine (Fisher, ACS certified, resublimed). This iodine was frozen with liquid nitrogen and pumped to evacuate. The iodine tube was attached to the four-probe vessel holding the $[CH]_x$ and the latter was evacuated for at least 2 h. After doping to the desired level (vide infra), the four-probe apparatus was taken into the drybox, the reference piece weighed, and a strip cut off of the sample piece for study. The four-probe was returned to the vacuum line and pumped for at least 30 min before the remaining samples were further doped. The error in determining the iodine content by weight change is less than 5%.

For samples doped with less than 0.1 mol % iodine, radioactive $^{125}I_2$ was used. Twenty milligrams of 100 μCi/mg of elemental $^{125}I_2$ (total activity = 2 mCi) was purchased from New England Nuclear in a 50-mL Pyrex bulb with a Teflon stopcock on the top and an O-ring joint on the side. Up to six weighed strips of $[CH]_x$ (2–5 mg) with identifying notches were placed in the four-probe, and samples were doped to the desired conductivity. The apparatus was opened in a glove bag in a hood, and a strip was placed in a 7-mm Pyrex tube for flame sealing and γ counting. The four-probe apparatus was returned to the vacuum line for evacuation and further doping. Samples were counted in duplicate in either a Packard Gamma Counter or Beckmann Gamma 4000 for 1 min. The counting efficiencies of the instruments were determined with a 0.101 μCi simulated I-125 standard (New England Nuclear). The mole fraction of dopant is calculated with

$$y = \frac{13.02Ca}{m \cdot \text{eff} \cdot f} \tag{1}$$

where C = counts per minute of doped polyacetylene, a = activity of iodine in disintegrations per minute/mole, m = mass of doped sample (g), f = correction for half-life, and eff = counter efficiency (cpm/dpm). The error of radioassay is about 5%.

During doping the vapor pressure of iodine[18] was controlled by use of cold baths. Initial doping was done with iodine at 195 K (dry ice/ethanol bath) or 250 K (carbon tetrachloride/liquid nitrogen slush), and the stopcock separating the iodine reservoir from the four-phase apparatus was opened for a short time of 5 s–5 min. These temperatures gave vapor pressures of less than 10^{-4} torr and 2.5×10^{-3} torr, respectively. The doping stopcock was closed, and the doped polyacetylene was pumped for 30–60 min. Samples were removed as previously described; the four-probe was evacuated for 30 min, and further doping was done. After 5 min of doping at 250 K, the conductivity increase was very slow, so the temperature of the iodine reservoir was raised to ca. 263–258 K with a sodium chloride/ice mixture, and when no further conductivity increase was observed, the temperature was raised to 273 K with an ice bath and then to room temperature. These temperatures gave iodine vapor pressures of ca. 10^{-2}, 3×10^{-2}, and 2.5×10^{-1} torr. This procedure is an improved version of one described earlier.[16] By choosing various iodine vapor pressures and doping times, we could accurately control the sample composition and conductivity.

Table I
Transport Properties of Pristine $[CH]_x$ at Room Temperature

		trans-$[CH]_x$	
M_n	*cis*-$[CH]_x$, σ, $(\Omega\ cm)^{-1}$	σ, $(\Omega\ cm)^{-1}$	$\mathcal{S}$, $\mu V\ K^{-1}$
500	$(2.6 \pm 1.6) \times 10^{-9}$	$(1.5 \pm 0.8) \times 10^{-5}$	1260 ± 440
10 500	$(2.5 \pm 1.6) \times 10^{-11}$	$(2.0 \pm 2.0) \times 10^{-6}$	
10 500[a]	3.0×10^{-10}	1.8×10^{-6}	1450 ± 150
100 000	4.0×10^{-11}	1.5×10^{-6}	
210 000	3.1×10^{-11}	1.1×10^{-6}	
270 000	5.4×10^{-10}	9.1×10^{-6}	2000 ± 200
870 000		4.1×10^{-6}	2000 ± 200
500[b]	1.8×10^{-9}	8.3×10^{-6}	1020

[a] References 5, 11. [b] $[CD]_x$.

Temperature-Dependent Conductivity. Conductivity at low temperature was measured with an Air Products LT-3-110 Heli-Tran system using the sapphire cell and an APD-E Model 3700 Digital temperature indicator/controller. Temperature calibration was checked with a Au (7% Fe) vs. chromel thermocouple and a Leeds and Northup 8686 mV potentiometer. One end of the Heli-Tran transfer line extends into a 40-L liquid nitrogen dewar with a rubber seal to allow pressurization, and the other end is inserted in the vacuum shroud that holds the sample.

Sample mounting was done in the drybox. The polyacetylene film was placed under two wires and against a sapphire disk in the vacuum shroud, and the wires were attached to the film with Electrodag. The sapphire provides the means for heat transfer, since measurements were made under vacuum. After evacuation for 1 h to 4×10^{-5} torr, cool down of the cell began, which reached 85 K within 90 min. The temperature was controlled to ±0.1 K by adjusting the heater power and nitrogen flow. Stable temperature and resistance readings were achieved within 5 min after setting, and data were taken every 4 K up to 299 K.

The resistance of the sapphire was 6×10^{10} Ω, thus limiting experiments to samples with lower resistances. Since the sample and sapphire were in parallel, they both contributed to the total resistance when they had comparable resistivities. The actual resistance of the sample is given by

$$R_{[CH]_x} = \left[\frac{1}{R_{\text{measured}}} - \frac{1}{R_{\text{sapphire}}} \right]^{-1} \tag{2}$$

This correction extended useful data to slightly lower temperatures. However, the lowest temperature of measurement is limited to that at which $R_{\text{measured}} \sim R_{\text{sapphire}}$.

A computer program was used (CDC FORTRAN EXTENDED Version 4) to aid in preparing plots of resistance vs. various functions of temperature. Temperature and log R data sets were entered; the output was a table of T, $T^{-1/4}$, $T^{-1/2}$, log T, $1/T$, and log R followed by the slope, y intercept, and correlation coefficient for each plot. The best fits were found by using an unweighted least-squares subroutine.

Other Measurements. Methods for the measurements of thermopower coefficient[5] and unpaired spin concentration[11] have been given previously.

Results

Pristine $[CH]_x$. A number of *cis*-$[CH]_x$ with different MW had been prepared; their σ_{RT} are given in Table I. The values for **L**-$[CH]_x$ are the average for four preparations isomerized under conditions ranging from 20 min at 423 K to 10 min at 463 K. The data of **S**-$[CH]_x$ are an average of three polymerizations isomerized variously for 4 h at 418 K to 17 min at 517 K. The variability of σ_{RT} for both the cis and trans isomer of **L**-$[CH]_x$ is small. However, even though **S**-*cis*-$[CH]_x$ can be prepared within a narrow range of σ_{RT}, the isomerized samples have con-

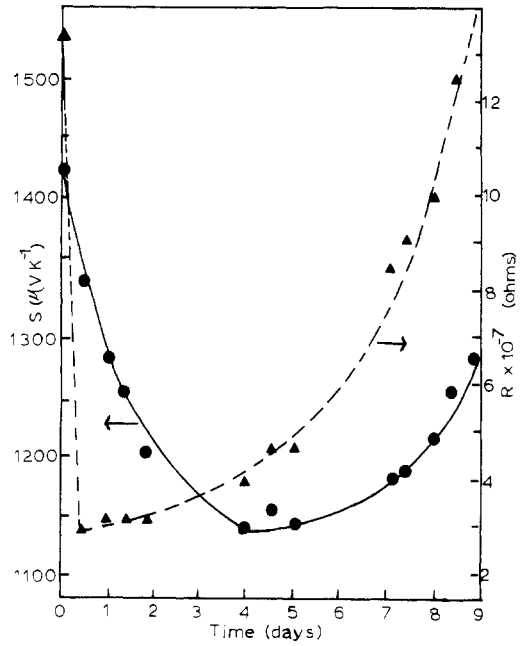

Figure 1. Variation of resistance (▲, dashed line) and thermopower (●, solid line) of **S**-*trans*-$[CH]_x$ with exposure time to air at room temperature.

ductivities varying from 2 to 50 × 10^{-7} $(\Omega\ cm)^{-1}$. The reproducibility of σ_{RT} for undoped **H**-*trans*-$[CH]_x$ seems to improve with the increase in MW.

We have investigated the possibility that extensive handling of the specimen with opportunities for contamination, especially by oxygen, could contribute to the variability in σ_{RT}. A procedure was described in the experimental section of polymerizing $[CH]_x$ film directly on the wires of a four-probe apparatus so that its conductivity can be measured without handling the polymer. *cis*-$[CH]_x$ polymerized on the four-probe at 195 K, washed 15 times with pentane, and warmed to room temperature had σ_{RT} of 3.6 and 6.0 × 10^{-9} $(\Omega\ cm)^{-1}$ for two runs. These values are much larger than those given in Table I. During washing the conductivity changed only slightly, increasing by a factor of 3 in the first case and by a factor of 1.2 in the second. Sample 1 was heated under vacuum at 423 K for 1 h, and then the temperature was gradually increased to 458 K over the next 50 min until a resistance minimum was reached. After the sample was cooled to room temperature, the conductivity was 6 × 10^{-5} $(\Omega\ cm)^{-1}$. Sample 2 was heated at 423 K for 210 min until a resistance minimum was reached; the σ_{RT} = 1.1 × 10^{-5} $(\Omega\ cm)^{-1}$. Again these values are more than 10 times greater than those in Table I. Therefore, handling the sample and brief exposure to air cannot account for the small and variable σ_{RT} for the **S**-*trans*-$[CH]_x$ samples because oxygen can act as a dopant to $[CH]_x$ during short exposure. Figure 1 shows that the exposure of a **S**-*trans*-$[CH]_x$ sample to air caused a decrease of resistivity of 10-fold in 1 h and 10^{10}-fold within 8 h, which is followed by slow return to the original resistivity after 8 days.

The variability in the σ_{RT} of **S**-*trans*-$[CH]_x$ may be partly attributed to incomplete isomerization or differences in morphological changes due to isomerization. **L**-$[CH]_x$ isomerizes completely in a single-stage process (Figure 2); the same seems to be true for very high MW **H**-$[CH]_x$-(87), as shown in Figure 3. By comparison, the **S**-$[CH]_x$ samples have an initial rapid increase in σ but slow down to a second stage of steady further increase in σ, as given in Figure 4 for five isomerization temperatures. It seems that for intermediate MW $[CH]_x$ in order to obtain optimum

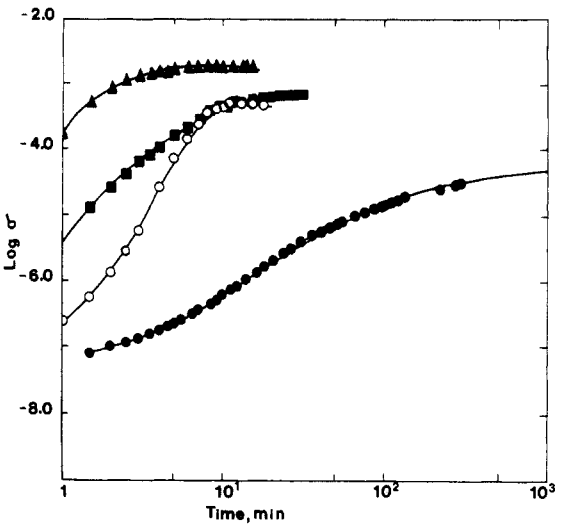

Figure 2. Variation of conductivity with time of isomerization for **L**-$[CH]_x$ at (●) 383 K, (■) 423 K, (▲) 453 K, and for **L**-$[CD]_x$ at (○) 453 K.

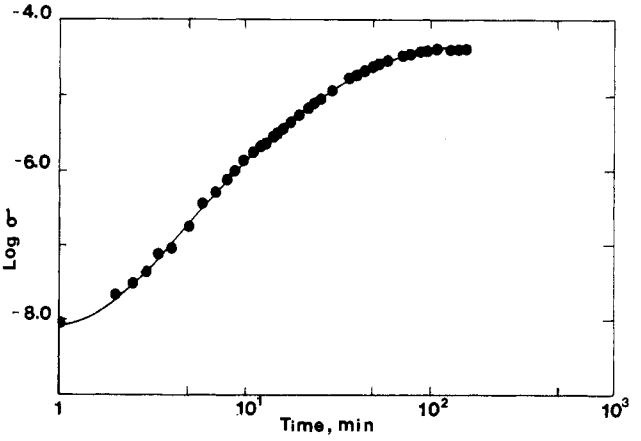

Figure 3. Variation of conductivity with time of isomerization for **H**-$[CH]_x$-(87) at 413 K.

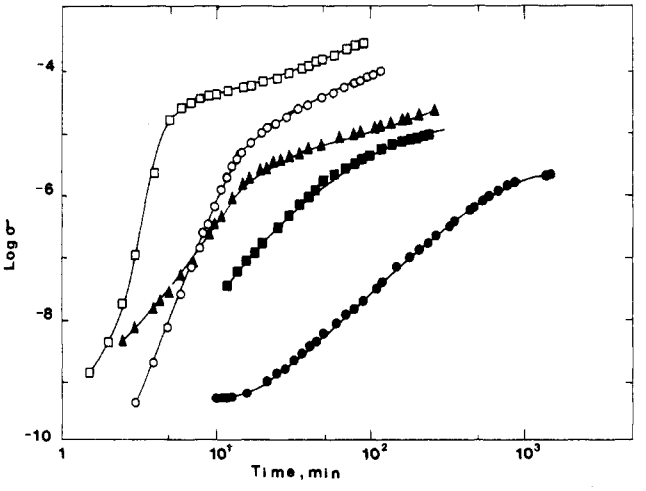

Figure 4. Variation of conductivity with time of isomerization for **S**-$[CH]_x$ at (●) 383 K, (■) 418 K, (▲) 423 K, (○) 441 K, (□) 468 K.

isomerization to maximum conductivity it should be performed with a control sample on the four-probe monitoring the process.

Within the experimental uncertainties mentioned, the results in Table I do show that both **L**-*cis*-$[CH]_x$ and **L**-*trans*-$[CH]_x$ have higher σ_{RT} than the higher MW samples. Certainly the $\mathcal{S}_{RT}$ values of **L**-*trans*-$[CH]_x$ are significantly

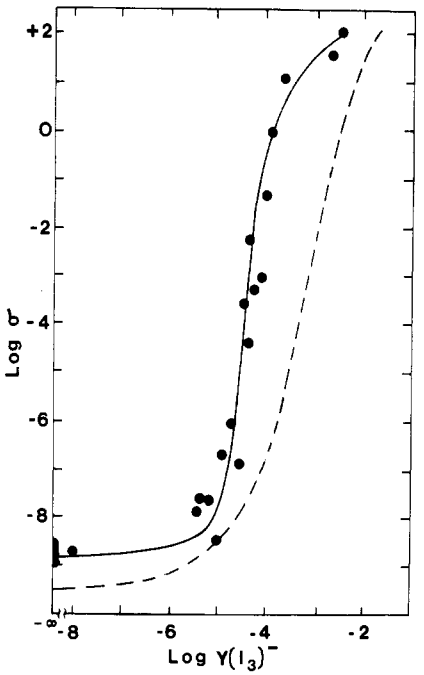

Figure 5. Increase of σ_{RT} with I_2 doping for L-*cis*-$[CH]_x$; dashed line is for S-*cis*-$[CH]_x$.[5]

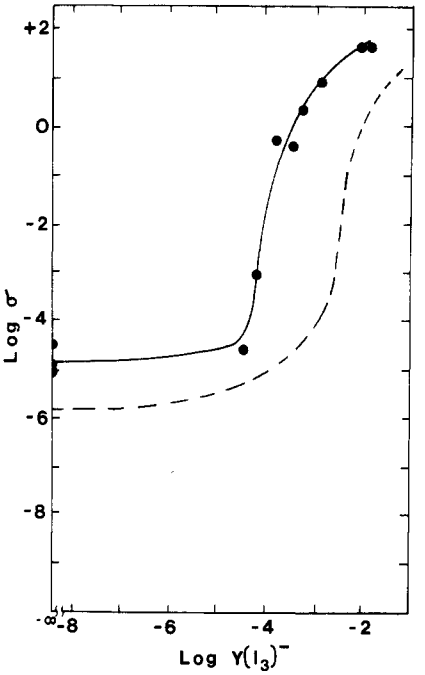

Figure 6. Increase of σ_{RT} with I_2 doping for (●) L-*trans*-$[CH]_x$; broken line is for S-*trans*-$[CH]_x$.[5]

lower than those of the other polymers.

Doped $[CH]_x$. L-*cis*-$[CH]_x$ was doped with iodine to $10^{-6} < y < 0.3$. The extensive data are given in Figure 5; the previously published result for S-*cis*-$[CH]_x$[5] is shown as the dashed curve. There is a very significant difference between the two polymers. The midpoint for the carrier "glass" transition in L-*cis*-$[CH]_x$ occurs at $y_m(I_3^-) \sim 3 \times 10^{-5}$, while y_m is about 3×10^{-4} for S-$[CH]_x$.

Similar doping curves for L-*trans*-$[CH]_x$ are given in Figure 6, including three samples of L-*trans*-$[CD]_x$. The results for S-*trans*-$[CH]_x$[5] are included for comparison. The differences for the two MW materials parallel those of the cis isomers. Dopant has no effect on σ of the low MW polymer until $y \geq 3 \times 10^{-5}$; whereas σ of S-$[CH]_x$ begins to increase at $y \sim 10^{-4}$. The $M_n = 500$ samples have

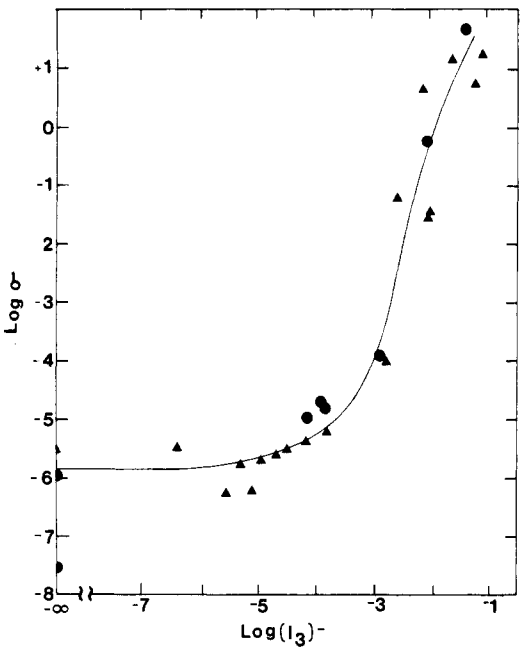

Figure 7. Increase of σ_{RT} with I_2 doping for *trans*-$[CH]_x$: (▲) $M_n = 11\,000$[5] and (●) $M_n = 210\,000$.

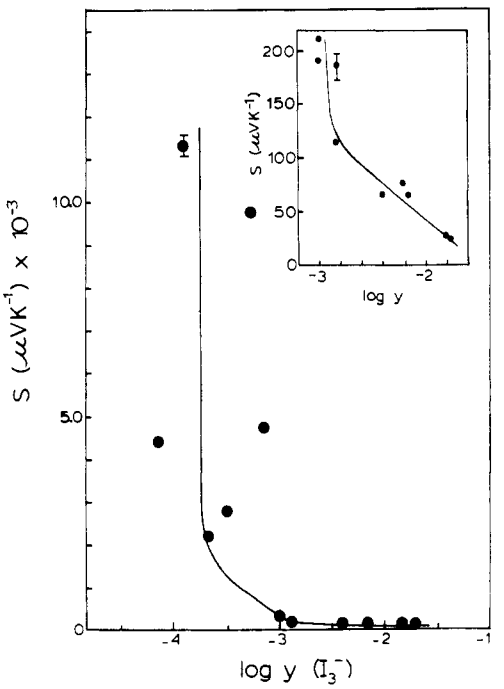

Figure 8. Variation of thermopower with y for S-*cis*-$[CH(I_3)_y]_x$. Insert shows details at high doping levels.

higher σ_{RT} than the $M_n = 11\,000$ polymer at all values of y. The mobility transition in L-*trans*-$[CH]_x$ occurs at $y_m \sim 8 \times 10^{-5}$ and over a narrower range of y than S-*trans*-$[CH]_x$.

The high MW $[CH]_x$ polymers have doping curves virtually superimposable to that of S-$[CH]_x$. Figure 7 shows the σ_{RT} for S-*trans*-$[CH(I_3)_y]_x$[5] and $M_n = 210\,000$ *trans*-$[CH(I_3)_y]_x$.

Previously,[5] we have observed very sharp drops of $\mathcal{S}$ with doping of S-*trans*-$[CH]_x$. This is now affirmed for the corresponding cis polymer with $M_n = 11\,000$ (Figure 8). The carrier "glass" transition has $y_m \sim 1.6 \times 10^{-4}$. The scatter of data is greater for the cis polymer than the previous data for the trans isomer. The thermopower doping curve for L-*trans*-$[CH]_x$ (Figure 9) is consistent with the conductivity doping curve of this polymer. The

Table II
Temperature-Dependent Conductivity[a] for Iodine-Doped S-*trans*-$[CH]_x$

		log T		$T^{-1/4}$		$T^{-1/2}$		T^{-1}	
sample no.	y	temp, K[b]	slope[c]	temp, K[b]	slope[c]	temp, K[b]	slope[c]	temp, K[b]	slope,[c] eV
1	2.6×10^{-6}	207	18.2	207	124	213	248	220	0.4
2	6.6×10^{-6}	207	15.6	204	110	210	213	238	0.35
3	1.3×10^{-5}	169	15.0	200	100	203	196	222	0.32
4	7.9×10^{-4}	166	11.7	177	78	197	131	222	0.26
5	1.05×10^{-3}	109	11.1	166	74	166	139	221	0.23
6	2.2×10^{-3}	91	7.3	197[d]	47		curved[e]	221	0.16
7	4.4×10^{-3}	88	5.0	202[f]	36	222	74.4	221	0.15
8	5.3×10^{-3}	168	4.4	114	26.7	180	15.8	200	0.09
9	1.4×10^{-2}	234[g]	1.4		curved[e]	199[h]	26.6	133	0.042

[a] Plots of log R vs. log T, $T^{-1/4}$, $T^{-1/2}$, T^{-1}. [b] Plot is linear between 295 K and indicated temperature. [c] Slope for the linear region. [d] Between 84 and 197 K the slope is 38. [e] Plot has continuous curvature. [f] Between 88 and 175 K the slope is 29. [g] Between 85 and 115 K the slope is 4.2. [h] Between 86 and 160 K the slope is 9.6.

Table III
Temperature-Dependent Conductivity[a] for Iodine-Doped S-*cis*-$[CH]_x$

		log T		$T^{-1/4}$		$T^{-1/2}$		T^{-1}	
sample no.	y	temp, K[b]	slope[c]	temp, K[b]	slope[c]	temp, K[b]	slope[c]	temp, K[b]	slope,[c] eV
10	5×10^{-4}	234	77			244	139	238	0.21
11	1.3×10^{-3}	85	5.0	98	30.9	160	61	217	0.10
12	1.6×10^{-3}	130	5.4	105	33	192	72	221	0.13
13	5.9×10^{-3}	curved[d]		curved[d]		curved[d]			

[a] Plots of log R vs. log T, $T^{-1/4}$, $T^{-1/2}$, and T^{-1}. [b] Plot is linear between 295 K and indicated temperature. [c] Slope for the linear-region. [d] Plot has continuous curvature.

$\mathcal{S}$ values remain unchanged with doping until $y \geq 10^{-4}$, and then it decreases sharply to the metallic value at $y \sim 3 \times 10^{-3}$. The midpoint of transition is at about 7×10^{-4}, which is almost identical to the y_m value for S-*trans*-$[CH]_x$ polymer.

H-*trans*-$[CH]_x$-(87) was isomerized from the cis polymer of M_n = 870 000 at 453 K for 20 min. Overnight doping with iodine yielded a doping level of $y(I_3^-) = 3 \times 10^{-2}$, $\sigma_{RT} = 10\ (\Omega\ cm)^{-1}$, and $\mathcal{S}_{RT} = +75\ \mu V\ K^{-1}$.

Temperature Dependence of Conductivity. The motivation for measuring $\sigma(T)$ is to test the functional dependencies for various mechanisms of electronic conduction. Therefore, it is desirable to measure σ to as low a temperature as possible. But there is limitation both in the measuring device and in the resistivity of the specimen. The Heli-Tran sapphire disk, which acts as heat-transfer sample holder, has a resistance of $6 \times 10^{10}\ \Omega$. Therefore, the resistivity of a $[CH]_x$ sample greater than $6 \times 10^9\ \Omega$ cannot be measured. This limitation becomes unimportant as $[CH]_x$ is doped and conductivity increases. In lieu of giving numerous figures, most of the data are presented in tabular form giving the slope of the linear region from 295 K to the lowest stated temperature below which the data deviates from linearity.

The $\sigma(T)$ results for S-*trans*-$[CH(I_3)_y]_x$ are given Table II. The undoped polymer has $R > 6 \times 10^9\ \Omega$ at 250 K; the data are linear for all the functional forms. Moses et al.[19] measured conductivity of S-*trans*-$[CH]_x$ down to 140 K; the log σ vs. $T^{-1/4}$ and log σ vs. log T plots both deviate from linearity at 151 K. Less extensive measurements by Epstein et al.[9b] showed deviation at 220 K for these plots.

For samples with $y \geq 6.6 \times 10^{-6}$, the various $R(T)$ plots deviate from linearity at the indicated temperatures in Table II, when the sample resistivities are much less than the instrument limit. However, for samples 1–4, the low temperatures for deviation are within 30 K for the different $R(T)$ plots, which cannot be considered as significant. The $R(T)$ data for samples 5–7 give power-law plots that are linear over the broadest temperature range. For $y = 1.05 \times 10^{-3}$ (Figure 10) the power-law plot is linear for about 60 K more than the other plots. For $y = 4.4 \times 10^{-3}$ the log R vs. $T^{-1/4}$ plot changes slope at ca. 190 K.

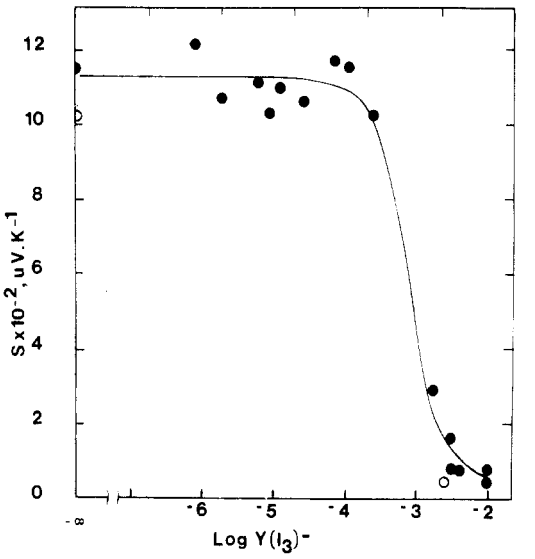

Figure 9. Variation of thermopower with y for (●) L-*trans*-$[CH(I_3)_y]_x$; (○) the perdeuterated polymer.

The log R vs. T^{-1} plots for samples 1–7 are inferior to all the other functional plots, usually linear only between 220 and 295 K. However, for the highly doped samples 8 and 9 the Arrhenius plots are superior to the others.

Because of the high resistivity of *cis*-$[CH]_x$, it was only possible to measure $R(T)$ at appreciable levels of doping. The limited data are given in Table III.

The temperature dependence of resistivity was measured for undoped L-*trans*-$[CH]_x$. The power-law plot has an exponent of 11.7, which reflects the higher σ_{RT} of this undoped polymer than the higher MW materials. The plot is linear over the temperature range measured from 295 to 108 K. The log R vs. $T^{-1/4}$ plot is linear down to 132 K with a slope of 70; below this temperature R increases more slowly with decreasing temperature. The log R vs. $T^{-1/2}$ plot is linear to 112 K with a slope of 135. The plot of log R vs. T^{-1} is linear to 213 K with an activation energy

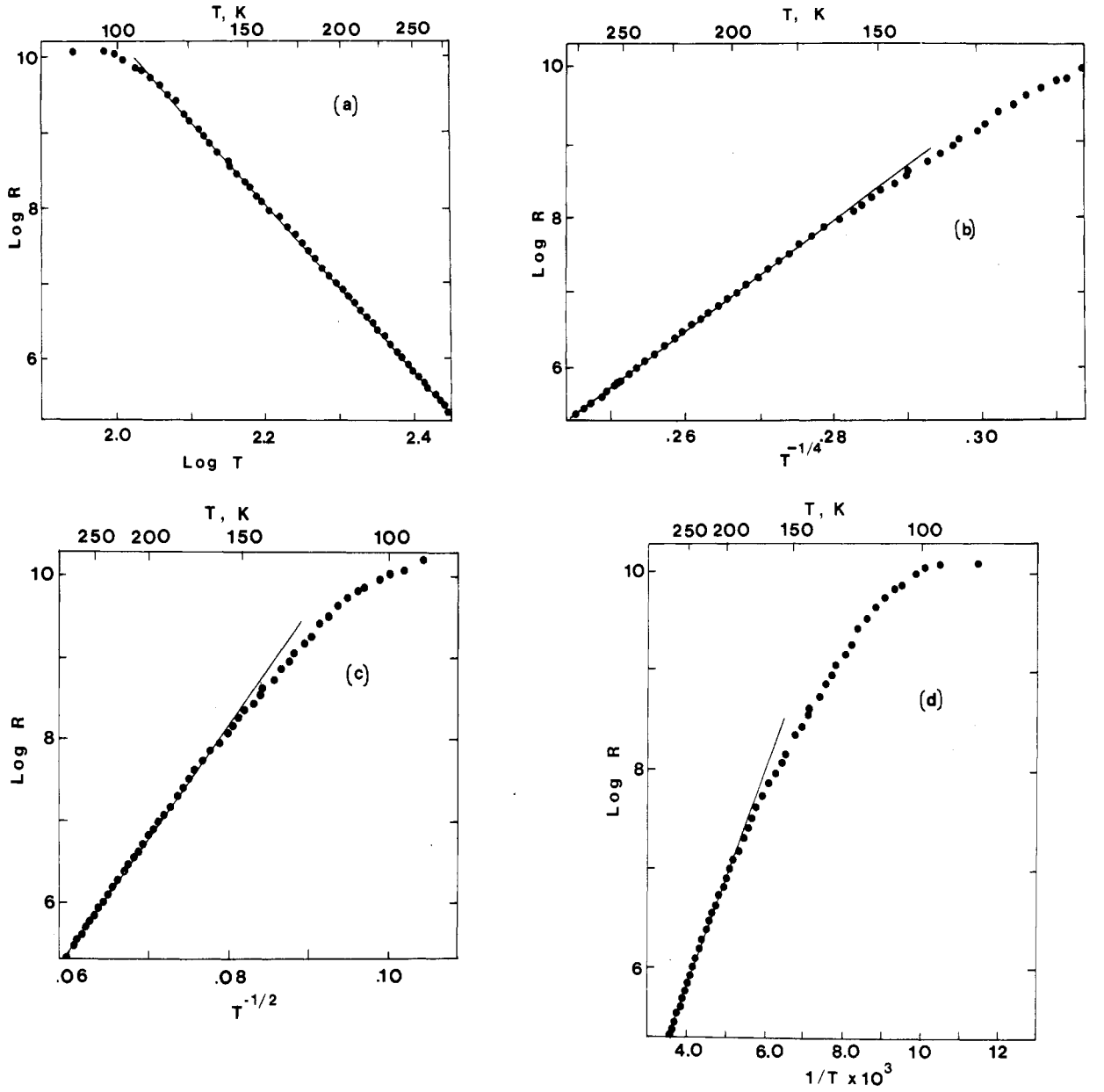

Figure 10. Temperature variation of log R for S-*trans*-$[CH(I_3)_{1.05\times10^{-3}}]_x$ vs. (a) log T, (b) $T^{-1/4}$, (c) $T^{-1/2}$, (d) T^{-1}.

of 0.29 eV. All these parameters are virtually identical with sample 4 of Table II, which is S-*trans*-$[CH]_x$ doped to $y(I_3^-) = 7.9 \times 10^{-4}$.

The $R(T)$ of M_n = 25 000 *trans*-$[CH]_x$ was also determined. The power-law plot has a slope of 15.5 for the linear region between 245 and 200 K. The slope is 108 from 295 to 208 K for the log R vs. $T^{-1/4}$ plot; it is 201 for the log R vs. $T^{-1/2}$ plot with deviation below 214 K. These values of the functional parameters are close to the undoped S-*trans*-$[CH]_x$.

Discussion

Effect of Dopant Concentration on Temperature-Dependent Conductivity. It will be inappropriate to survey completely the usage of $\sigma(T)$ or $R(T)$ data to deduce conduction mechanism. A few citations would suffice to illustrate this endeavor. Epstein et al.[9] and Moses et al.[19] found good fits for both log R vs. $T^{-1/4}$ and log T for undoped S-*trans*-$[CH]_x$. The slope of the former plot was 100 times larger than typically found for amorphous semiconductors The authors favored the IEH model[20] because the observed power-law exponent was 13–14, which is close to the theoretical value of 11. Also there is an $\omega^{0.8}$ dependence for ac conductivity in accordance with the IEH model. The power-law plot of *trans*-$[CH]_x$, which was lightly iodine-doped to an unknown concentration, has the same slope as the power-law plot for the undoped polymer.[9b] Epstein et al.[9] concluded that IEH applies to lightly doped *trans*-$[CH]_x$ as well. It should be noted that contact problems could give spurious results at high frequencies.[21] Early on, we have pointed out[1] that the $\sigma(T)$ data, such as those reported by Epstein et al.[9b] for NH_3-compensated *trans*-$[CH]_x$, can be analyzed equally well by the power law with an exponent of 17.9, by Arrhenius plot with an activation energy of 1.1 eV, and by $T^{-1/4}$ dependence giving $\sigma(T) \propto \exp[-(2.5 \times 10^{-11}/T)^{1/4}]$.

The $\sigma(T)$ studies of doped polyacetylene are made difficult by possible artifacts due to doping. Audenart et al.[10c] prepared several samples of *trans*-$[CHI_y]_x$. Two samples with y = 0.11 and 0.19 have $\sigma(T)$ for 3-D variable range hopping (VRH);[22] two other samples with y = 0.29 and 0.03 have $\sigma(T)$ consistent with FIT mechanism.[23] For two heavily doped specimens of *trans*-$[CHI_y]_x$ cut from the same doped film, Epstein et al.[10a] observed one to have resistivity depending logarithmically with temperature and the other behaving as conduction by 3-D VRH. Ehringer

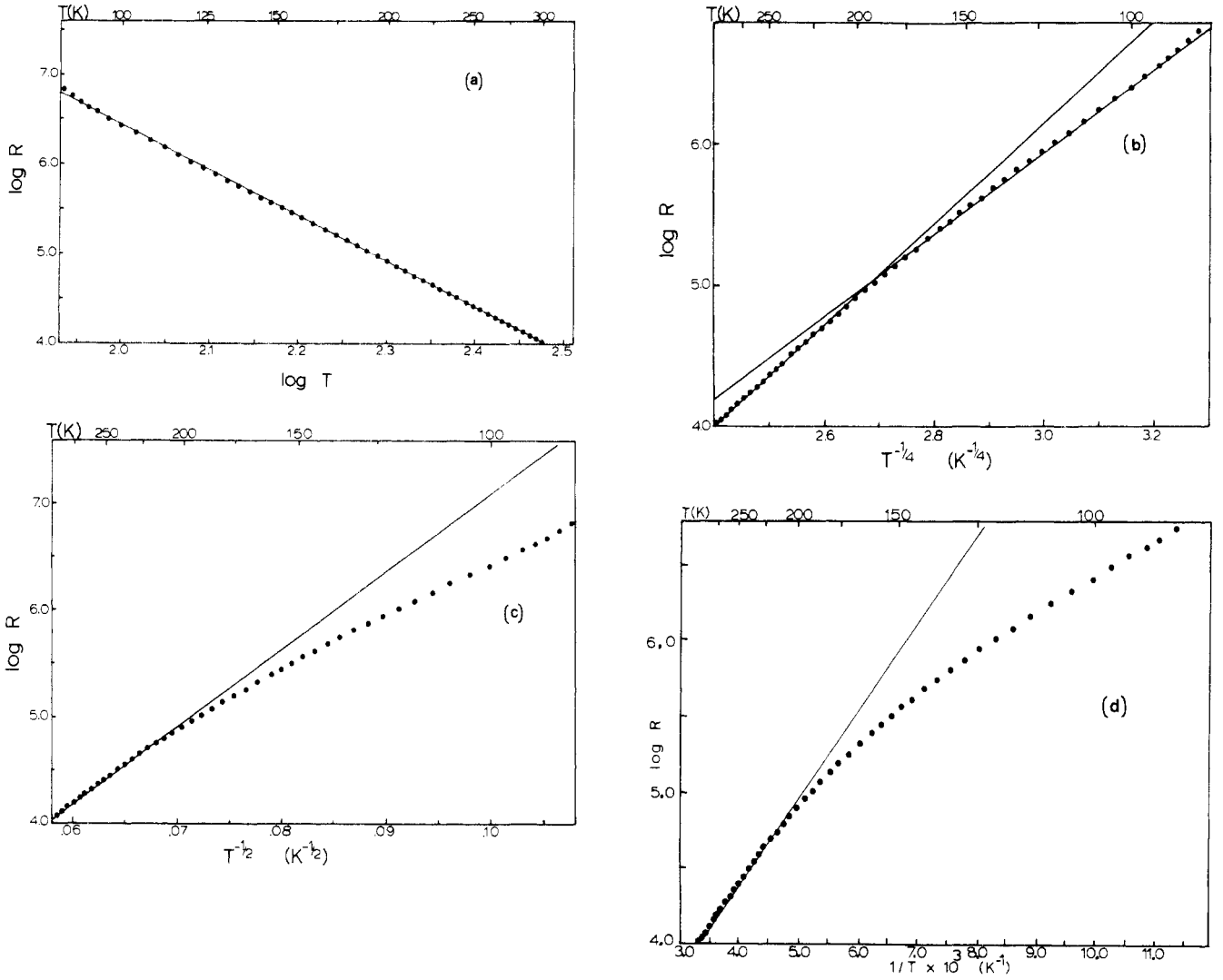

Figure 11. Temperature variation of log R for S-*trans*-$[CH(I_3)_{4.4\times10^{-3}}]_x$ vs. (a) log T, (b) $T^{-1/4}$, (c) $T^{-1/2}$, (d) T^{-1}.

et al.[10b] studied $\sigma(T)$ for *trans*-$[CH(I_3)_y]_x$ and concluded conduction by 1-D VRH for $y < 0.05$ on the basis of the linear log σ vs. $T^{-1/2}$ plot, 3-D VRH for $0.05 < y < 0.15$ because of log $\sigma(T^{-1/4})$ behavior, and material to be dirty metal for $y > 0.15$ which displays a $\sigma \sim T^{\nu}$ dependence. Earlier, Chiang et al.[4a] found that iodine doped samples with $0.043 < y < 0.0063$ have nearly linear plots of log σ vs. either $T^{-1/4}$ or $T^{-1/2}$. Sichel et al.[22a] found *cis*-$[CH(I_3)_y]_x$ samples to show linear log σ vs. $T^{-1/4}$ plots for $y = 2.5$, 3.3, and 7.0×10^{-3} and concluded conduction by 3-D VRH. These authors[22] doped *cis*-$[CH]_x$ with various agents to $10^{-2} \leq y \leq 10^{-1}$. For iodine and bromine, log R vs. $T^{-1/4}$ dependence was found, and for $IrCl_6$ and AsF_5 log R vs. $T^{-1/2}$ plots were found to be linear. The attributed this difference to the cylindrical geometry of I_3^- and Br_3^- ions in contrast to the large octahedral geometry of $IrCl_6^{-2}$ and AsF_6^- dopant ions. For *cis*-$[CH]_x$ doped with $FeCl_3$ the authors found a temperature dependence of log R intermediate between $T^{-1/2}$ and $T^{-1/4}$. Finally, a linear log $(\sigma T^{1/2})$ vs. $T^{-1/4}$ plot has been said to indicate conduction via VRH among soliton states for *trans*-$[CH]_x$ doped with $FeCl_3$[8] ($3 \times 10^{-3} < y < 0.0185$) and doped with iodine to nearly metallic state[24] ($0.01 < y < 0.05$). In other papers by Epstein et al.[10] the authors concluded that for $y(I_3^-) > 0.05$ charge transport is characterized by disordered metallic behavior.

It is imprudent to draw hasty conclusions regarding the mechanism of conduction based on the conductivity dependence on temperature alone. Our study showed that all the commonly considered temperature dependencies described the data over a smaller or larger temperature range. Even for samples 6–8 in Table II, which obey the power law to the temperature limit of our measurements, deviation may occur at lower temperatures. Looking at all the data in Table II, one would favor the power-law dependence except for the nearly metallic sample 9, which seems to favor an exponential dependence.

The fact that our $R(T)$ data can be best described by power law should not be taken to support the IEH model. In the intersoliton electron hopping mechanism, the temperature and dopant concentration terms can be factored. Kivelson[20] made seven predictions of IEH, two of which are particularly relevant here: (1) dopant concentration does not affect the temperature dependence of conductivity, and (2) conductivity varies with temperature due to electron–phonon coupling as $\sigma\alpha(T)^{x+1}$ where $x = 10$. These two criteria were cited by Moses et al.[19] and Epstein et al.[9] to declare conduction by ISH for undoped and lightly doped *trans*-$[CH]_x$. Our results showed that T and y cannot be factored because the power-law exponent varies strongly with y. In polyacetylene approximately one charge carrier is formed by each dopant ion.[25] Hopping between the localized states depends upon the average distance separating them in space, which is proportional to $y^{1/3}$. Figure 12 shows that the power-law exponents d vary linearly with $y^{1/3}$ for iodine-doped *trans*-$[CH]_x$.

A second evidence against IEH is that the power-law dependence of log σ vs. log T also appears to be the best

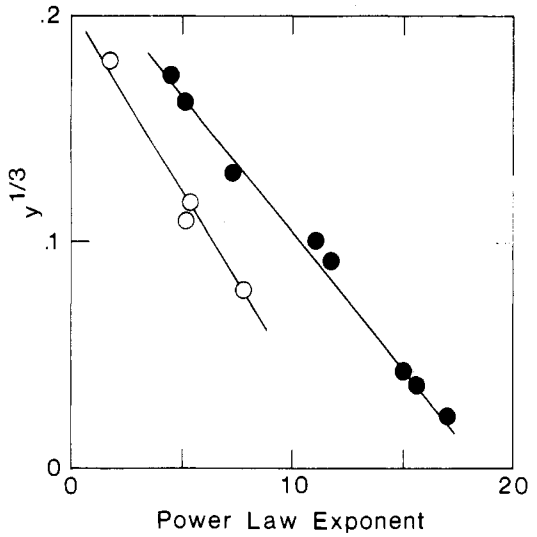

Figure 12. Variation of power-law exponent d vs. $y^{1/3}$ for (●) **S**-*trans*-$[CH(I_3)_y]_x$; (○) **S**-*cis*-$[CH(I_3)_y]_x$.

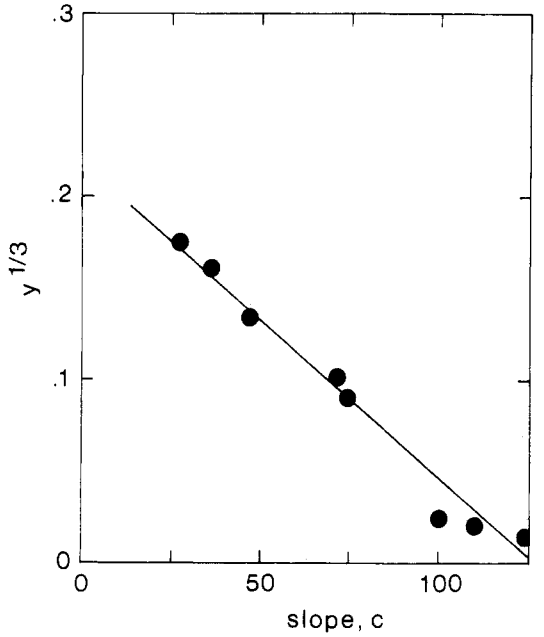

Figure 13. Variation of slope c in log σ vs. $T^{-1/4}$ plots with $y^{1/3}$ for **S**-*trans*-$[CH(I_3)_y]_x$.

compared with the other $\sigma(T)$ plots for **S**-*cis*-$[CH(I_3)_y]_x$ (Table III) as well. It is a basic axiom[26] that soliton excitation can only exist in *trans*-$[CH]_x$, not in *cis*-$[CH]_x$. This shows that the power-law relationship needs not to be related to models of conduction involving solitons. Figure 12 also shows that the power-law exponent varies linearly with $y^{1/3}$ for the iodine-doped cis polymer, though the data are more limited to higher doping levels than the trans isomer system.

The general importance of the effect of dopant on temperature-dependent conductivity can be seen in Figures 13 and 14. The slopes a, b, and c for the log R vs. T^{-1}, $T^{-1/2}$, and $T^{-1/4}$, respectively, all bear linear relationship to $y^{1/3}$.

Effect of Molecular Weight. Various properties of $[CH]_x$ with a wide range of MW have been compared. The very low MW polymer, **L**-$[CH]_x$, has the same cis crystal structure as the higher MW polymers **H**-$[CH]_x$ but is less ordered along the **c**-axis.[14] It is isomerized to the trans structure, having probably a more compact unit cell than **H**-$[CH]_x$, with apparent annealing of crystallite which increases the longitudinal order during thermal isomerization. These processes occur more readily and with lower activation energy for **L**-$[CH]_x$ than for **H**-$[CH]_x$. The *trans*-$[CH]_x$ has the same unpaired spin concentration of 4.8×10^{-4}/CH regardless of MW,[16] which is affected identically by doping. **L**-*trans*-$[CH]_x$ has narrower EPR linewidth and longer T_1 than the higher MW polymers; however, doping with I_2 has the same effects on T_1 and T_2 of the polymers independent of MW. Therefore, the spin dynamics[16] is not influenced by the overall length of the polymer backbone.

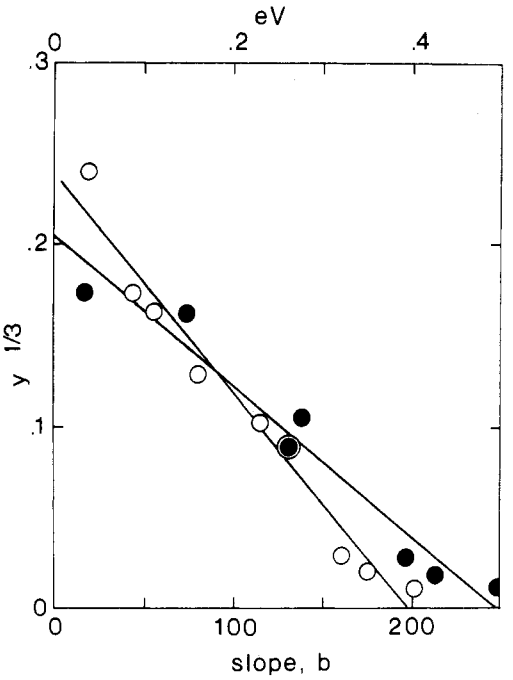

Figure 14. Variation of (●) slope b in log σ vs. $T^{-1/2}$ plots and of (○) slope a in log σ vs. T^{-1} plot with $y^{1/3}$ for **S**-*trans*-$[CH(I_3)_y]_x$.

The pristine **L**-$[CH]_x$ have greater σ_{RT} than the corresponding cis and trans polymers with higher MW. The thermopower coefficient of *trans*-$[CH]_x$ increases with increasing MW. The temperature-dependent conductivity of **L**-*trans*-$[CH]_x$ resembles closely that of the $M_n = 11000$ polymers doped to $y(I_3^-) = 7.9 \times 10^{-4}$.

Carrier Transport Mechanisms. The simplicity of polyacetylene structure and the fact that it was the first organic polymer to be doped to metallic conductivity makes it the widely accepted model for conducting polymers. A number of properties of $[CH]_x$ have been explicitly or tacitly assumed to be important for electronic conduction such as crystalline morphology, long conjugated backbone, electronically degenerate ground state or high molecular symmetry, moving defect domains (neutral or charged soliton), etc. We have synthesized several homopolymer and copolymer systems and compared their properties with $[CH]_x$ in order to scrutinize those structural features though to be indispensable for electronic conduction. We give first a brief description of these systems.

Acetylene–methylacetylene copolymers of a wide range of compositions have been synthesized.[27] They are completely amorphous materials with varying shades of greenish-gold coloration. Undoped copolymers containing 45 mol % of $CH_3C{\equiv}CH$ have EPR line widths comparable to the corresponding isomers of $[CH]_x$. Upon doping with iodine this copolymer has about one third of the σ_{RT} of iodine-doped $[CH]_x$. The copolymer and $[CH]_x$ differ greatly in the degree of backbone conjugation by virtue of the dissimilarity of the two backbone carbon atoms in the methylacetylene unit. Therefore, carrier transport is not strongly dependent on a structure of fully conjugated

backbone having slight differences in bond lengths, as in the case of *trans*-$[CH]_x$. Furthermore, properties such as EPR line widths which had been used to support the soliton excitation model in *trans*-$[CH]_x$ and absence of it in *cis*-$[CH]_x$ cannot be valid because analogous differences exist in the two isomeric forms of acetylene–methyl acetylene copolymers.

We have synthesized acetylene–carbon monoxide copolymers[28] with up to 13 mol % of the CO monomer having an average structure of 6 –CH=CH– units separated by a –C(=O)– unit that interrupts the backbone conjugation. The pristine copolymers have no crystallinity or fibrillar morphology and have fewer unpaired spin than *cis*-$[CH]_x$. The unpaired spin concentration, [S·], *decreases* upon thermal isomerization of the copolymer to 10^{-4}–10^{-3} of the numbers in *trans*-$[CH]_x$.[29] In spite of the low [S·], the undoped copolymers have σ_{RT} and $\mathcal{S}_{RT}$ values comparable to the corresponding $[CH]_x$ samples. Doped copolymers are nearly as conductive as similarly doped $[CH]_x$ homopolymers.

Poly(monocyanoacetylene) and poly(dicyanoacetylene) have been compared;[30] the former should have strongly alternating backbone bonds, and the latter has identical backbone carbon atoms as in *trans*-$[CH]_x$ and may be expected to have the associated Peierls instability, weak bond alternation, degenerate ground state, and diffusive defects. Yet the two amorphous polymers have the same undoped and doped magnetic properties and conductivities.

Since all the above copolymers are amorphous, neither crystallinity nor fibrillar morphology is very important to electrical conductivity. The results of acetylene–methylacetylene copolymers showed that a fully conjugated backbone π-system is not an essential requirement for conduction. The fact that undoped and doped electrical conductivities of acetylene–carbon monoxide copolymers are greater or comparable to the respective polyacetylenes suggests that frequent interruption of the backbone conjugation is not severely detrimental. It seems that the π-system may be as short as $(–CH=CH–)_6$. The main function of the π-system is to provide low-energy molecular orbitals to permit redox or electrochemical doping and to stabilize the resulting charge carriers which are delocalized carbanions or carbocations.

There is now ample evidence that unpaired spins, whether they are freely diffusing or not, have nothing to do with electrical conductivity. The *trans* acetylene–carbon monoxide copolymers have very few unpaired spins, yet they have $\mathcal{S}_{RT}$ and σ_{RT} comparable to *trans*-$[CH]_x$. Some analogues of poly(phenylene vinylene)[31] have very large [S·] but are nearly insulators, while others have small [S·] but appreciable conductivity. In the case of *trans*-$[CH]_x$, as doping begins to increase σ, there is a concomitant sharp decrease in [S·].[11] For *cis*-$[CH]_x$, [S·] was much smaller than for the trans-isomer; doping increases that value to about 10^{-4} as compared to [S·] = 4.8×10^{-4} in undoped *trans*-$[CH]_x$. However, the cis polymer has doped conductivity greater than that of the trans polymer at the same dopant concentrations for $y(I_3^-) > 10^{-4}$. Consequently, any conduction mechanism invoking the participation of unpaired spins is probably not viable.

For some time it was generally accepted[4] that the semiconductor to metal transition occurs at a few percent doping, accompanied by the emergence of Pauli susceptibility.[32] We[5] and Moses et al.[6] realized that the very large increase of conductivity and decrease in thermopower occur at a very low dopant concentration of $y \sim 7 \times 10^{-4}$ for both AsF_5 and I_2 doping. The large increase of σ_{RT} occurs by about 100-fold increase in y in the case of **S**-$[CH]_x$ but occurs over much smaller increase in y for **L**-$[CH]_x$ (Figures 5 and 6). The changes in $\mathcal{S}_{RT}$ vs. dopant concentration are much sharper than those of σ_{RT} (Figure 8). In *p*-type doped $[CH]_x$, the charge carriers are the delocalized carbocations. We have pointed out[5,30] that they are strongly pinned, i.e., immobilized, by the Coulomb force of the counterion, and they may be said to be in a "glassy" state, implying very low mobility. As dopant concentration increases, the pinning potential tends to decrease due to shielding effect. It was proposed that at y_m there is nearly complete shielding of the pinning potential and that a charged carrier can interact equally and weakly with two or more counterions. We believed that there is a dramatic increase in carrier mobility via 3-D variable range hopping at this point and coined the terms carrier mobility transition or carrier "glass" transition. At $y \gg y_m$ further doping has mainly the effect of increasing the number of carriers but only slight effect of enhancing the carrier mobility. What we are saying is that the rigorous and restrictive concepts of soliton or polaron excitation, though intellectually appealing, are irrelevant to the electrical conductivities of the rapidly expanding variety of polymers, some of which may not even require doping.[33]

According to the above model, temperature and dopant-concentration effects on transport cannot be factored. The determinant is the average distance separating the charge carriers and between their counterions. Large separation would require greater energy for carrier hopping. This is the explanation for the $y^{1/3}$ dependence of the slopes of various $R(T)$ plots (Figures 12–14). A possible mechanism of carrier hopping had been proposed elsewhere.[30]

Acknowledgment. This work was supported in part by grants from NSF and ONR.

Registry No. *cis*-$[CH]_x$, 25768-70-1; *trans*-$[CH]_x$, 25768-71-2; I_2, 7553-56-2.

References and Notes

(1) Chien, J. C. W. "Polyacetylene-Physics, Chemistry, and Material Sciences"; Academic Press: New York, 1984.
(2) MacDiarmid, A. G.; Heeger, A. J. *Synth. Met.* **1979/80**, *1*, 101.
(3) (a) Park, Y. W.; Denenstein, A.; Chiang, C. K.; Heeger, A. J.; MacDiarmid, A. G. *Solid State Commun.* **1979**, *29*, 745. (b) Park, Y. W.; Heeger, A. J.; Druy, M. A.; MacDiarmid, A. G. *J. Chem. Phys.* **1980**, *73*, 946.
(4) Variation of log σ_{RT} vs. y had been reported for the following dopants: (a) I_2 and Br_2. Chiang, C. K.; Gau, S. C.; Fincher, C. R., Jr.; Park, Y. W.; MacDiarmid, A. G.; Heeger, A. J. *Appl. Phys. Lett.* **1978**, *33*, 18. Chiang, C. K.; Park, Y. W.; Heeger, A. J.; Shirakawa, H.; Louis, E. J.; MacDiarmid, A. G. *J. Chem. Phys.* **1978**, *69*, 5098. (b) AsF_5. Chiang, C. K.; Fincher, C. R., Jr.; Park, Y. W.; Heeger, A. J.; Shirakawa, H.; Louis, E. J.; Gau, S. C.; MacDiarmid, A. G. *Phys. Rev. Lett.* **1977**, *39*, 1098. (c) SbF_5. Rolland, M.; Bernier, P.; Disi, M.; Linaya, C.; Sledz, J.; Schue, F.; Fabre, J. M.; Giral, L. *J. Phys., Lett.*, **1980**, *41*, L165. (d) WCl_6, $MoCl_5$, CF_3SO_3H. Rolland, M.; Aldissi, M.; Schue, F. *Polymer* **1982**, *23*, 834. (e) BF_3, H_2SO_4, $ClSO_3H$. Watanabe, A.; Tanaka, M.; Tanaka, J. *Chem. Lett.* **1980**, 575. (f) Na. Francois, B.; Mermilliod, N.; Zuppiroli, L. *Synth. Met.* **1981**, *4*, 131. Chung, T. C.; Moraes, F.; Flood, J. D.; Heeger, A. J. *Phys. Rev. B: Condens. Matter* **1984**, *29*, 2341.
(5) Chien, J. C. W.; Warakomski, J. M.; Karasz, F. E.; Chia, W. L.; Lillya, C. P. *Phys. Rev. B: Condens. Matter* **1983**, *28*, 6937.
(6) Moses, D.; Denenstein, A.; Chen, J.; Heeger, A. J.; McAndrew, P.; Woerner, T.; MacDiarmid, A. G.; Park, Y. W. *Phys. Rev. B: Condens. Matter* **1982**, *25*, 7652.
(7) Kwak, J. F.; Gill, W. D.; Greene, R. L.; Seeger, K.; Clarke, T. C.; Street, G. B. *Synth. Met.* **1979**, *1*, 213.
(8) Przybylski, M.; Bulka, B. R.; Kulszeuicz, I.; Pron, A. *Solid State Commun.* **1983**, *48*, 893.
(9) (a) Epstein, A. J.; Ronmelmannr, H.; Abkowitz, M.; Gibson, H. W. *Phys. Rev. Lett.* **1981**, *47*, 1549. (b) *Mol. Cryst. Liq. Cryst.* **1981**, *77*, 81.

(10) (a) Epstein, A. J.; Gibson, H. W.; Chaikin, P. M.; Clark, W. G.; Grüner, G. *Chem. Scr.* **1981**, *17*, 135. *Phys. Rev. Lett.* **1980**, *45*, 1730. (b) Ehringer, E.; Bauhofer, W.; Menke, K.; Roth, S. *J. Phys., Colloq.* **1983**, *44*, 63–115. (c) Audenart, M.; Gusman, G.; Deltour, R. *Phys. Rev. B: Condens. Matter* **1981**, *24*, 7380.
(11) Chien, J. C. W.; Wnek, G. E.; Karasz, F. E.; Warakomski, J. M.; Dickinson, L. C. *Macromolecules* **1982**, *15*, 614.
(12) (a) Chien, J. C. W.; Capistran, J. D.; Karasz, F. E.; Dickinson, L. C.; Schen, M. A. *J. Polym. Sci., Polym. Lett. Ed.* **1983**, *21*, 93. (b) Chien, J. C. W.; Karasz, F. E.; Schen, M. A.; Hirsch, J. A. *Macromolecules* **1983**, *16*, 1694.
(13) (a) Wnek, G. E.; Capistran, J.; Chien, J. C. W.; Dickinson, L. C.; Gable, R.; Gooding, R.; Gourley, K.; Karasz, F. E.; Lillya, C. P.; Yao, K. D. In "Conductive Polymers"; Seymour, R. B., Ed.; Plenum: New York, 1981; pp 183–208. (b) Schen, M. A.; Karasz, F. E.; Chien, J. C. W. *J. Polym. Sci., Polym. Chem. Ed.* **1983**, *21*, 2787. (c) Chien, J. C. W.; Schen, M. A. *Makromol. Chem., Rapid Commun.*, in press.
(14) Chien, J. C. W.; Schen, M. A. *J. Polym. Sci., Polym. Chem. Ed.*, in press.
(15) Schen, M. A.; Karasz, F. E.; Chien, J. C. W. *Makromol. Chem., Rapid Commun.* **1984**, *5*, 217.
(16) Chien, J. C. W.; Schen, M. A. *Macromolecules*, in press.
(17) Ito, T.; Shirakawa, H.; Ikeda, S. *J. Polym. Sci., Polym. Chem. Ed.* **1974**, *12*, 11.
(18) (a) Weast, R. C.; Ed. "CRC Handbook of Chemistry and Physics", 55th ed.; CRC Press: Cleveland, OH, 1974; pp D-162, D-190. (b) Menzies, A. W. C.; In "International Critical Tables of Numerical Data, Physics, Chemistry and Technology"; Washburn, E. W., Ed.; McGraw-Hill, New York, 1928; Vol. III, p 201.
(19) Moses, D.; Chen, J.; Denenstein, A.; Kaveh, M.; Chung, T. C.; Heeger, A. J.; MacDiarmid, A. G. *Solid State Commun.* **1981**, *40*, 1007.
(20) (a) Kivelson, S. *Mol. Cryst. Liq. Cryst.* **1981**, *77*, 65. (b) *Phys. Rev. Lett.* **1981**, *46*, 1344. (c) *Phys. Rev. B: Condens. Matter* **1982**, *25*, 3798.
(21) (a) Lakaho, A. L.; Abkowitz, M. *Phys. Rev. B: Solid State* **1971**, *3*, 1791. (b) Street, R. A.; Davies, G.; Yoffe, A. D. *J. Non-Cryst. Solids* **1971**, *5*, 276.
(22) Mott, N. F. *Philos. Mag.* **1970**, *22*, 7.
(23) Sheng, P. *Phys. Rev. B: Condens. Matter* **1980**, *21*, 2180.
(24) (a) Epstein, A. J.; Rommelmann, H.; Bigelow, R.; Gibson, H. W.; Hoffman, D. M.; Tanner, D. B. *J. Phys., Colloq.* **1983**, *44*, C3-61. (b) *Phys. Rev. Lett.* **1983**, *50*, 1866.
(25) (a) Hsu, S. L.; Signorelli, A. J.; Pez, G. P.; Baughman, R. H. *J. Chem. Phys.* **1978**, *69*, 106. (b) Kaindl, G.; Wortmann, G.; Roth, S.; Menke, K. *Solid State Commun.* **1982**, *41*, 75.
(26) (a) Su, W. P.; Schrieffen, J. R.; Heeger, A. J. *Phys. Rev. Lett.* **1979**, *42*, 1698. (b) *Phys. Rev. B: Condens. Matter* **1981**, *22*, 2099.
(27) Chien, J. C. W.; Wnek, G. E.; Karasz, F. E.; Hirsch, J. A. *Macromolecules* **1981**, *14*, 479.
(28) Chien, J. C. W.; Babu, G. N. *Macromolecules* **1985**, *18*, 622.
(29) (a) Chien, J. C. W.; Babu, G. N. *J. Chem. Phys.* **1985**, *82*, 441. (b) Chien, J. C. W.; Babu, G. N.; Hirsch, J. A. *Nature (London)* **1985**, *314*, 723.
(30) (a) Chien, J. C. W.; Carlini, C. *Makromol. Chem., Rapid Commun.* **1984**, *5*, 597. (b) Chien, J. C. W.; Carlini, C. *J. Polym. Sci., Polym. Chem. Ed.* **1984**, *22*, 2749. (c) Chien, J. C. W.; Carlini, C. *J. Polym. Sci., Polym. Chem. Ed.* **1985**, *23*, 1383.
(31) (a) Wnek, G. E.; Chien, J. C. W.; Karasz, F. E.; Lillya, C. P. *Polymer* **1979**, *20*, 1441. (b) Gourley, K. D.; Lillya, C. P.; Reynolds, J. R.; Chien, J. C. W. *Macromolecules* **1984**, *17*, 1025.
(32) (a) Ikehata, S.; Kaufer, J.; Woerner, T.; Pron, A.; Druy, M. A.; Sivak, A.; Heeger, A. J.; MacDiarmid, A. G. *Phys. Rev. Lett.* **1980**, *45*, 1123. (b) Epstein, A. J.; Rommelmann, H.; Druy, M. A.; Heeger, A. J.; MacDiarmid, A. G. *Solid State Commun.* **1981**, *38*, 683.
(33) Reynolds, J. R.; Karasz, F. E.; Lillya, C. P.; Chien, J. C. W. *J. Chem. Soc., Chem. Commun.* **1985**, 268.

Sulfur Trioxide Doped Poly(phenylene sulfide)

Karl F. Schoch, Jr.,* James F. Chance, and Kenneth E. Pfeiffer

Westinghouse Research and Development Center, Pittsburgh, Pennsylvania 15235.
Received April 12, 1985

ABSTRACT: Sulfur trioxide doping of poly(phenylene sulfide) produces a material with an electrical conductivity as high as 10^{-4} S/cm at room temperature. Samples of poly(phenylene sulfide) films were exposed to SO_3 at various pressures between 26 and 260 torr at room temperature. Although the samples were hygroscopic after doping, they did not decompose on exposure to air. In addition to raising the conductivity of the polymer, SO_3 also changed the structure of the polymer itself, possibly by sulfonation or cross-linking or both. Elemental analyses were consistent with the dopant species being SO_3^{2-}. X-ray diffraction of films before and after doping showed that doping induced substantial disorder in the polymer, possibly the result of incorporation of dopant between chains or of cross-linking.

Introduction

Since the discovery of high conductivity in polyacetylene,[1] much work has been done to understand the reasons for its high conductivity and to investigate the electrical properties of other polymers, such as polypyrrole,[2] poly(phenylene sulfide),[3] poly(phenylene),[4] pyrolyzed poly(acrylonitrile),[5] poly[(phthalocyaninato)siloxanes,[6] etc. A limitation of many of the systems, including polyacetylene, has been their poor stability toward ambient conditions. In particular, some are readily oxidized by oxygen in the air, and some of the common dopants are decomposed by moisture.

Our efforts have been directed at preparing materials with greater stability than those commonly available. One of the polymers we have worked with extensively is poly(phenylene sulfide) (PPS). Its attractive properties include its excellent thermal stability, relatively simple processing characteristics, and the fact that it is commercially available. PPS melts at 300 °C without decomposition and can be made into films and fibers from the melt. The polymer is quite crystalline after annealing, and its changes on annealing have been thoroughly characterized.[7] Doping of the polymer with AsF_5 has been investigated extensively by groups at Allied, IBM, and GTE.[3,8] The doped polymer has a conductivity of 1 S/cm at room temperature, but the conductivity can be as high as 25 S/cm if doping is carried out in AsF_3 solution.[9] During doping the polymer is believed to undergo some cross-link formation that changes the relative orientations of the polymer chains, increasing the planarity of the system.[3a] As with any AsF_5-doped system, however, this doped polymer is extremely moisture-sensitive. Many other common dopants, which are more stable to ambient conditions, are not sufficiently strong oxidizing agents to oxidize PPS and raise the con-

0024-9297/85/2218-2389$01.50/0